AN AIRCRAFT FUSELAGE FRACTURE ANALYSIS

Thiago A. A. Oliveira
Gilberto Gomes
Eng.thiagoarnaud@gmail.com
Ggomes2007@
University of Brasília
Asa Norte, SQN 406, Bloco K, Ap. 208, Brasília, Brazil

Abstract.

The continuum mechanics deals with the interaction between two bodies in order to analyze the stresses in the domain due to the contact load. In this way, to compute the stresses, it is considered each body as a semi-infinite in extent and having a plane surface. The Boundary Element Method (BEM) appears as a numerical technique for evaluating this type of problem. Using this technique, the boundary is discretized and the stresses are computed in the body domain. This paper consists of the multiscale analysis via Dual Boundary Element Method (DBEM) of fatigue life of aircraft fuselage plate. The macro analysis is evaluated through the stress field in the plate due to continuum mechanics. With this stress field, a micro element, composed by different distribution of cracks, is subjected to fatigue and analyzed by Dual Boundary Element Method (DBEM). This is accomplished using the software BemCracker2D obtaining fatigue life data in each crack increment. For this, advanced computational techniques were developed to evaluate the fracture mechanics behavior with the purpose of ensuring the integrity and the good functioning of the fuselage during its design lifespan.

Keywords: Dual Boundary Element Method, Multiscale Analysis, Fatigue, Aircraft Fuselage.

1 Introduction and Theory

From the technical point of view, it is sought to develop structures that are subject to combinations of external loads in a way that works in the usual situation and does not reach the respective Ultimate and Service Limit States [1]. For this, the knowledge of the stress field is a necessary condition to predict the behavior of these elements to avoid combinations that provoke a Limit State.

This paper analyzes the growth of aircraft fuselage subjected to external loads evaluated from the continuum mechanics [2]. In this way, a macro analysis of stresses in a fuselage plate is realized from the theory of the continuum, and after it is analyzed the behavior of the advance of the crack in this plate to evaluate fatigue, residual strength, Stress Intensity Factors, crack path and the deformations at every crack increase. The main objective is to evaluate from the continuum mechanics, cracked fuselage plates when subjected to continuum stresses. And, as specific objectives define crack propagation to obtain fracture mechanics parameters at each increment, such as: Stress Intensity Factors, number of loading cycles (fatigue), deformations and residual strength [3-12].

Fatigue is characterized by a cyclic loading process that causes progressive internal cumulative structural damage. After a certain number of cycles, the cracks can reach critical lengths that can make the structure unstable and, in some cases, lead to collapse. Admitting an elastic half-space body shown in Figure 1. External loads p(x) and q(x) act on the surface over the region from x = -a to x = b while the remainder of the body is free from loads. The stress components σ_x, σ_y, τ_{xy} at all points through the solid are computed according to [13, 14] shown in Equations 1, 2 and 3.

$$\sigma_x = -\frac{2y}{\pi}\int_{-a}^{b}\frac{p(s)(x-s)^2}{((x-s)^2+y^2)^2}ds - \frac{2}{\pi}\int_{-a}^{b}\frac{q(s)(x-s)^3}{((x-s)^2+y)^2}ds \tag{1}$$

$$\sigma_y = -\frac{2y^3}{\pi}\int_{-a}^{b}\frac{p(s)}{((x-s)^2+y^2)^2}ds - \frac{2y^2}{\pi}\int_{-a}^{b}\frac{q(s)(x-s)}{((x-s)^2+y^2)^2}ds \tag{2}$$

$$\tau_{xy} = -\frac{2y^2}{\pi}\int_{-a}^{b}\frac{p(s)(x-s)}{((x-s)^2+y^2)^2}ds - \frac{2y}{\pi}\int_{-a}^{b}\frac{q(s)(x-s)^2}{((x-s)^2+y^2)^2}ds \tag{3}$$

2 Methodology

To achieve the objectives a routine was developed in Matlab to automate the stress field derived from continuum mechanics based on [13, 14] and showed in Eqs. 1, 2 and 3. From the stress field, it is analyzed the crack propagation in an infinitesimal element through Dual Boundary Element Method (DBEM) using BemCracker2D [15, 16] to obtain the required parameters. The DBEM has several advantages over other methods, mainly due to the simplified modelling of the cracked area, direct SIF calculation, reduced run times and accurate crack growth simulation [17-19].

2.1 Macro element analysis

Figure 2 shows the model of the continuum problem to be analyzed. *P* and *Q* are normal and shear loads (MPa), respectively, and they can be non-uniform with lengths *a* and *b* (cm). With automation, loads *P*, *Q* (MPa) and *a*, *b* (cm) will assume the values in Table 1.

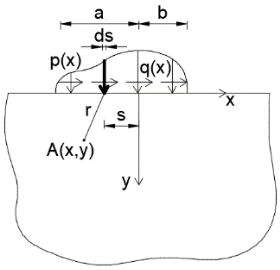

Figure 1: Model of the continuum mechanics

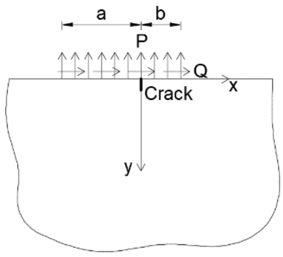

Figure 2: Macro element analysis

Table 1: Loading Series

	P	Q	a	b
Loading Series 1	1000	0	-10	10
Loading Series 2	1000	0	-10	0
Loading Series 3	1000	1000	-10	10
Loading Series 4	1000	1000	-10	0
Loading Series 5	0	1000	-10	10
Loading Series 6	0	1000	-10	0

2.2 Micro element analysis

From the applied external load, the micro element is subject to stress in the directions x (σ_x), y (σ_y), and shear (τ), according to Figure 3. The value is obtained directly from the stress field of Eqs. 1, 2 and 3 considering a square of 1 cm of side located in the origin of the axis (x, y) of Figure 2. The pre-established crack has initial size of 0.1 cm.

3 Results

For the 1 x 1 cm micro element located at the axis origin shown in Figure 2 with a preexisting crack of 0.1 cm size subjected to the loading series 1, 2 and 3 presents the following stress fields indicated in Table 2. Applying these stress fields, the crack growth path and deformation results are shown in Figures 4, 5, 6, 7 and 8 for each loading series, respectively. The objective results of this work are shown in Tables 3, 4, 5, 6, 7 and 8 for each increment of crack of size 0.05 cm.

Table 2: Stress field in the micro element (MPa)

Loads (MPa)	σ_x	σ_y	τ
Loading Series 1	999.87	1000.00	0.00
Loading Series 2	499.94	500.00	318.31
Loading Series 3	999.87	1000.00	999.87
Loading Series 4	0.00	818.31	818.25
Loading Series 5	0.00	0.00	999.87
Loading Series 6	0.00	318.31	499.94

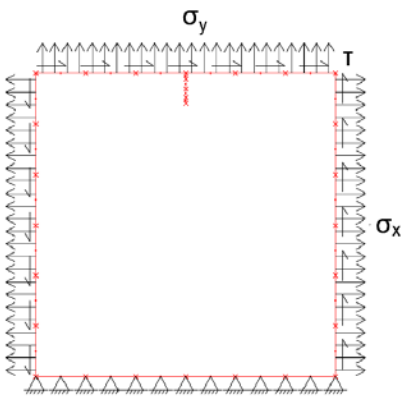

Figure 3: Micro element stress field

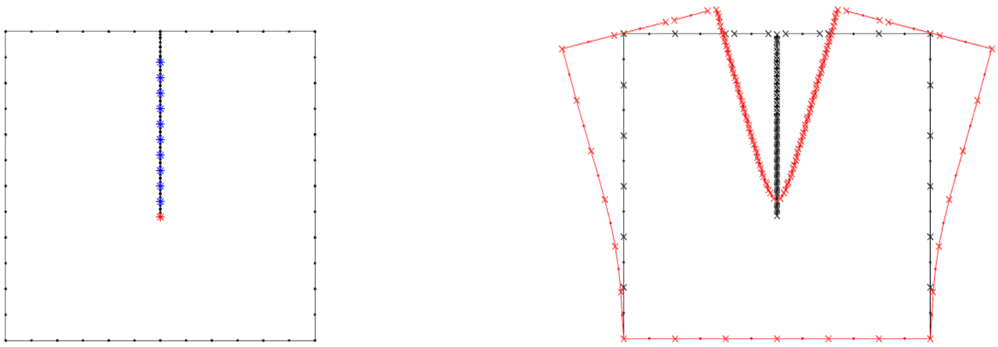

(a) Crack growth (b) Deformed mesh

Figure 4: Fuselage behaviour Loading Series 1

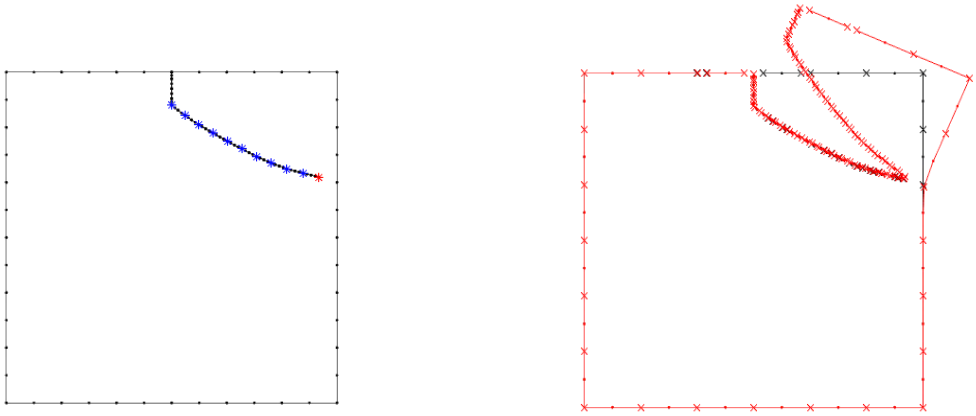

(a) Crack growth (b) Deformed mesh

Figure 5: Fuselage behaviour Loading Series 2

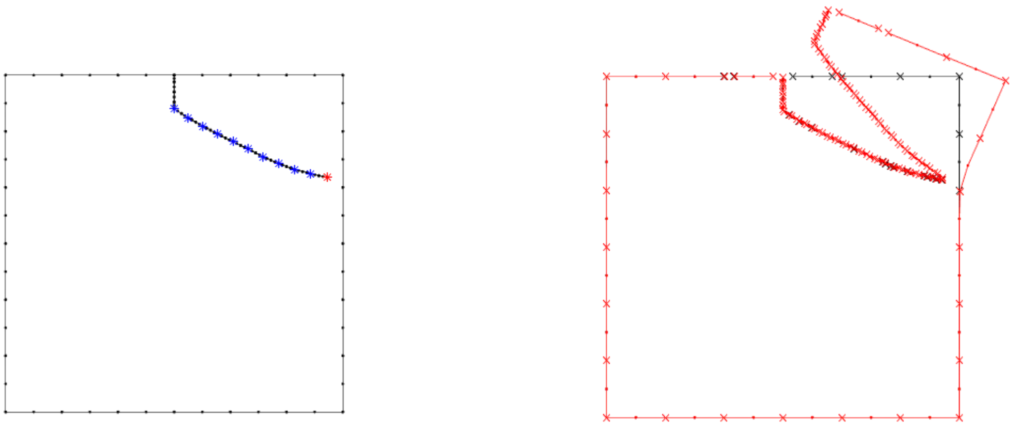

(a) Crack growth (b) Deformed mesh

Figure 6: Fuselage behaviour Loading Series 3

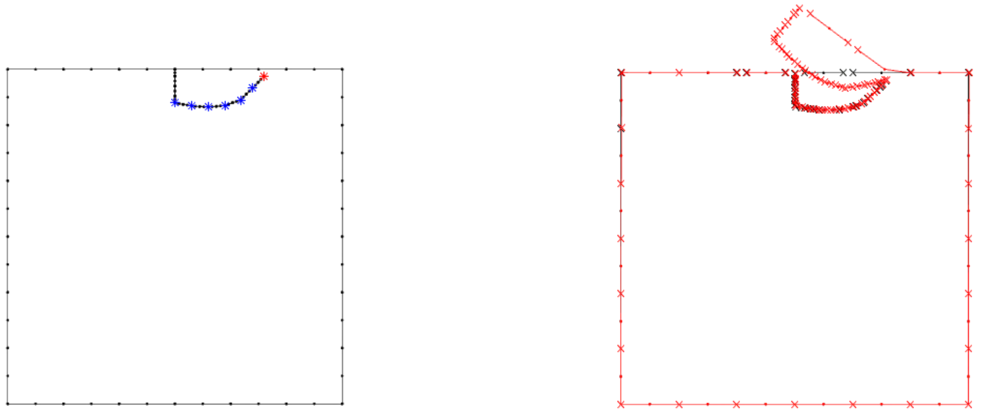

(a) Crack growth (b) Deformed mesh

Figure 7: Fuselage behaviour Loading Series 4

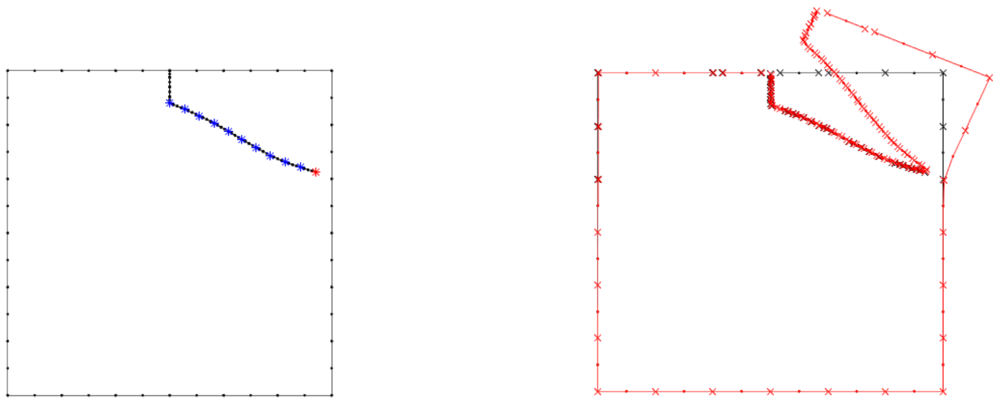

(a) Crack growth (b) Deformed mesh

Figure 8: Fuselage behaviour Loading Series 5

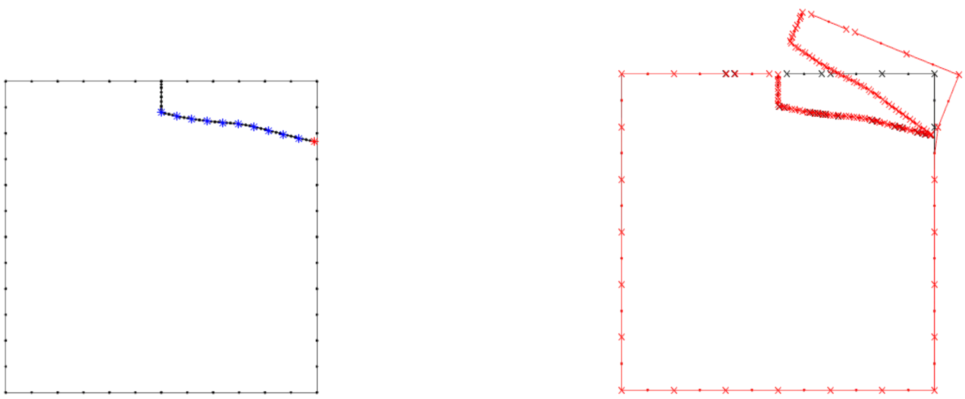

(a) Crack growth (b) Deformed mesh

Figure 9: Fuselage behaviour Loading Series 6

Table 3: Results for Loading Series 1

Crack increment	**Residual Strength**	**Load Cycles**	**SIF I (MPa√m)**	**SIF II (MPa√m)**	**SIF-EQ (MPa√m)**
0	0	0	72.0622	-1.99E-12	1
1	0.755681	52.49072	95.3607	3.87E-12	1.32331
2	0.599116	74.93781	120.281	5.71E-12	1.66913
3	0.488826	85.94768	147.419	3.49E-12	2.04572
4	0.407959	91.83705	176.641	5.77E-12	2.45122

5	0.347234	95.2159	207.532	9.02E-12	2.8799
6	0.300915	97.27797	239.477	1.13E-11	3.3232
7	0.265304	98.61077	271.621	1.43E-11	3.76926
8	0.237991	99.52177	302.793	1.37E-11	4.20183
9	0.217433	100.1813	331.422	1.50E-11	4.59911
10	0.202717	100.6895	355.482	1.77E-11	0

Table 4: Results for Loading Series 2

Crack increment	Residual Strength	Load cycles	SIF I (MPa√m)	SIF II (MPa√m)	SIF-EQ (MPa√m)
0	0	0	36.0315	-18.1037	1
1	0.632296	213.5569	73.2124	-0.84049	1.58154
2	0.462899	262.0393	99.9985	-1.30234	2.1603
3	0.352915	280.5802	131.166	-1.60581	2.83354
4	0.269149	288.3648	171.998	-1.84885	3.71541
5	0.200498	291.5654	230.901	-2.1395	4.98759
6	0.143529	292.7709	322.502	-4.36119	6.96725
7	0.097036	293.167	477.023	-6.43715	10.3055
8	0.060193	293.2741	769.099	-7.71436	16.6134
9	0.032617	293.2959	1419.23	-16.9419	30.6589
10	0.015239	293.2988	3037.89	-30.1767	0

Table 5: Results for Loading Series 3

Crack increment	Residual Strength	Load cycles	SIF I (MPa√m)	SIF II (MPa√m)	SIF-EQ (MPa√m)
0	0	0	72.0622	-56.8669	1
1	0.625724	12.19713	180.323	-2.97177	1.59815
2	0.457403	14.90175	246.723	-3.10891	2.18626
3	0.349803	15.9353	322.623	-3.83444	2.85875
4	0.267462	16.37333	421.986	-3.77599	3.73886
5	0.199112	16.55436	566.807	6.25634	5.02231
6	0.14179	16.62216	795.865	-11.0773	7.05268
7	0.094871	16.644	1189.55	-14.2971	10.5406
8	0.057789	16.6497	1953	-19.7375	17.3044
9	0.030269	16.65079	3728.16	-50.1163	33.037
10	0.014518	16.65092	7772.58	-112.564	0

Table 6: Results for Loading Series 4

Crack increment	Residual Strength	Load cycles	SIF I (MPa√m)	SIF II (MPa√m)	SIF-EQ (MPa√m)
0	0	0	-1.03274	-46.5369	1
1	0.462376	58.17771	114.887	-3.02649	2.16274
2	0.295878	68.5422	179.651	-2.94942	3.37977
3	0.204239	71.15631	260.284	-3.69231	4.89622
4	0.13787	71.94176	385.551	-6.18795	7.25323
5	0.067592	72.13344	786.415	-12.7495	14.7947
6	0.023467	72.15182	2241.98	-190.739	0

Table 7: Results for Loading Series 5

Crack increment	Residual Strength	Load cycles	SIF I (MPa√m)	SIF II (MPa√m)	SIF-EQ (MPa√m)
0	0	0	5.26E-12	-56.8669	1
1	0.70775	42.85735	92.7189	-1.92455	1.41293

2	0.533504	66.2019	123.024	-2.15511	1.8744
3	0.41769	76.00086	157.148	-2.50916	2.39412
4	0.323276	80.4276	203.06	2.88698	3.09333
5	0.241713	82.31484	271.616	-2.89937	4.13714
6	0.172536	83.03004	380.51	4.25847	5.79588
7	0.116098	83.26259	565.396	-8.58928	8.61339
8	0.071527	83.32451	917.885	-9.54093	13.9807
9	0.038275	83.33682	1715.07	-24.0966	26.1266
10	0.018188	83.33842	3609.64	-40.1977	0

Table 8: Results for Loading Series 6

Crack increment	Residual Strength	Load cycles	SIF I (MPa√m)	SIF II (MPa√m)	SIF-EQ (MPa√m)
0	0	0.00E+00	-0.40058	-28.4337	1
1	0.535001	304.8075	60.9072	-1.49791	1.86915
2	0.364999	387.2771	89.3236	-1.39278	2.73973
3	0.271768	413.3057	119.968	-1.84095	3.67961
4	0.20842	423.7156	156.436	-2.29929	4.79799
5	0.158883	428.1429	205.199	3.25889	6.29394
6	0.115122	429.9184	283.155	-5.37929	8.68646
7	0.074583	430.5016	437.111	-7.33041	13.4078
8	0.040978	430.6351	795.669	11.3547	24.4033
9	0.018362	430.6535	1775.73	-25.0611	54.4615
10	0.011113	430.6551	2045.23	-1348.8	0

4 Conclusion

The crack paths follow the stress field presented in Table 2. Loading Series 1 result in a linear crack path due to the symmetrical stress field without shear stress. The crack growth in Loading Series 2 is similar to Loading Series 3 since the stress field is almost half of each other. Loading Series 4 and 6 represent a mixture of high and low magnitude of y-normal and shear stress, respectively. In the first case (LS4) the crack is deflected up. In Loading Series 5 there is the crack growth for pure shear stress.

Now, analyzing the numerical results of residual strength and load cycles in Tables 3 to 8 varying the size of application (LS1, LS3 and LS5 a=b=10 cm ; to LS2, LS4 and LS6 a=0 cm and b=10 cm), comparing the Loading Series 1 and 2 (Tables 3 and 4, respectively) with pure external normal stress (P=1000 MPa), neglecting the external shear load. The residual strength reduces and the number of load cycles increases since the micro stress field reduces. For Loading Series 3 and 4 there is a mixture of normal and shear loads (P=1000 MPa and Q=1000 MPa), in these case the residual strength reduces and the number of load cycles increases, again, since the micro stress field reduces. For Loading Series 5 and 6 with pure external shear load (Q=1000 MPa) residual strength reduces and the number of load cycles increases, again, since the micro stress field reduces.

Analyzing the results of Stress Intensity Factors (SIF), there is a mixed mode fracture and higher values of σ_x, σ_y and τ increases SIF I and SIF II depending on the crack direction. For Loading Series 1, SIF I increases and SIF II is zero for each crack propagation. In all other Loading Series both SIF I and SIF II increase for each crack increment.

Acknowledgements

The authors are grateful to the Brazilian National Research Council (CNPq), to the Brazilian Coordination for the Improvement of Higher Education (CAPES) and to Federal District Research Support Foundation (FAP-DF) for the supporting funds for this research.

References

[1] Melchers, R. E. Structural Reliability Analysis and Prediction. 2. ed. Chichester, United Kingdom: Wiley. 456 p, 1999.

[2] T. Oliveira, G. Gomes, F. Evangelista Jr. Multiscale aircraft fuselage fatigue analysis by the dual boundary element method. Multiscale aircraft fuselage fatigue analysis by the dual boundary element method. Engineering Analysis with Boundary Elements 104, 2019.

[3] T. L. Anderson, Fracture mechanics: Fundamentals ans Applications, Boca, Ed., CRC Press, 2005.

[4] D. Broek, The practical use of fracture mechanics, 1 ed., Netherlands: Kluwer Academic Publishers, 1988.

[5] Z. P. Bazant and J. Planas, "Fracture and size effect in concrete and other quasibrittle materials," CRC Press, 1998.

[6] P. C. Paris and F. Erdogan, "A critical analysis of crack propagation laws," Journal of basic engineering, nº 85, pp. 528-534, 1960.

[7] A. A. Griffith, "The phenomena of rupture and flow in solids," Philosophical Transactions of the Royal Society of London, vol. 221, pp. 163-198, 1921.

[8] A. A. Griffith, "The theory of rupture," First International Congress of Applied Mechanics, nº In C. B. Biezeno and J. M. Burgers, pp. 55-63, 1924.

[9] G. R. Irwin, "Analysis of stress and strain near the end of a crack traversing a plate," Journal of Applied Mechanics, vol. 24, pp. 361-364, 1957.

[10] G. R. Irwin, "Onset of Fast Crack Propagation in High Strength Steel and Aluminium Alloys," Sagamore Research Conferece Proceedings, vol. 2, pp. 289-305, 1956.

[11] J. R. Rice, "A path independent integral and the approximate analysis of strain concentration by notches and cracks," Journal of applied mechanics, vol. 35, pp. 379-386, 1968.

[12] J. R. Rice, "The mechanics of crack tip deformation and extension by fatigue," Syrup. on fatigue crack growth, nº ASTM-STP-415, 1967.

[13] Johnson K. L. *Continuum mechanic*, Cambridge University Press, 1985.

[14] Sackfield A., Hills D. A., Nowell D. *Mechanics of elastic continuums*, Butterworth-Heinemann, ISBN**:** 9781483291949, 45-48, 1993.

[15] G. Gomes and M.A.M. Noronha, A B-Rep data structure and object GUI programming to implement 2D boundary elements. International Journal of Applied Mathematics and Computation. 4 (2012) 369-381.

[16] G. Gomes, A. M. Delgado Neto and L. C. Wrobel, Modeling and view of 2D cracks using Dual Boundary Integral Equation (in Portuguese), Brasília/DF, Brazil, DF: Proceedings of the XXXVII Iberian Latin-American Congress on Computational Methods in Engineering, ABMEC/RIPE, 2(6), pp. 120-133, 2016, p. 113.

[17] A. Portela, M. H. Aliabadi and D. P. Rooke, "The Dual Boundary Element Method: Efective implementation for crack problems," International Journal for Numerical Methods in Engineering, vol. 33, pp. 1269-1287, 1992.

[18] A. Portela, M. H. Aliabadi and D. P. Rooke, "Dual boundary element analysis of cracked plates: singularity subtraction technique," International Journal of Fracture, vol. 55, pp. 17-28, 1993.

[19] G. E. Blandford, A. R. Ingraffea and J. A. Liggett, "Two-Dimensional Stress Intensity Factor Computations Using the Boundary Element Method," International Journal Numerical Methods in Engineering, nº 17, pp. 387-404, 1981.